IEEE Photonics Journal
An IEEE Photonics Society Publication

Two Photon Emission and Nonlinear Optical Imaging of Acetonitrile-Treated Quasi-Spherical Nanoscale PbS Systems

Volume 2, Number 6, December 2010

N. Dutta
D. Mohanta
G. A. Ahmed
A. Choudhury
R. Hristu
S. G. Stanciu
G. A. Stanciu

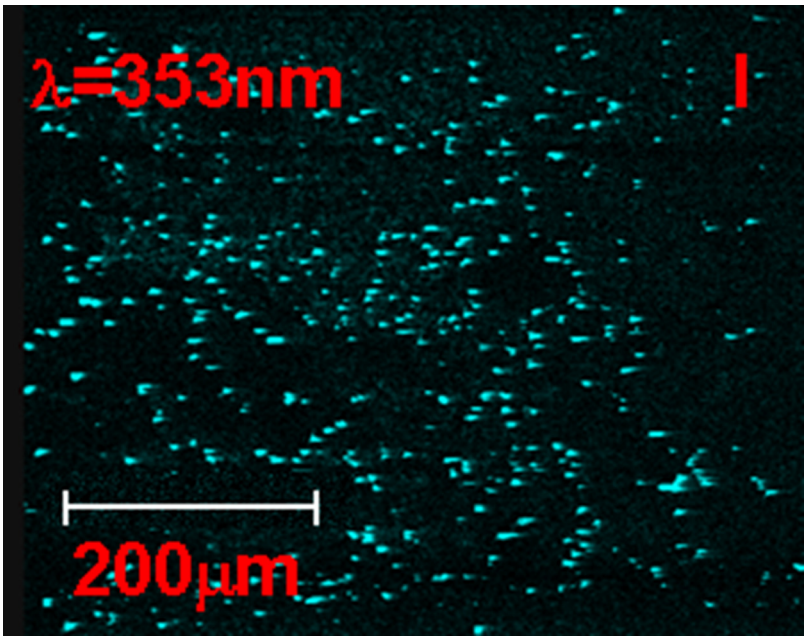

DOI: 10.1109/JPHOT.2010.2093513
1943-0655/$26.00 ©2010 IEEE

IEEE photonics SOCIETY
IEEE

Two Photon Emission and Nonlinear Optical Imaging of Acetonitrile-Treated Quasi-Spherical Nanoscale PbS Systems

N. Dutta,[1] D. Mohanta,[1] G. A. Ahmed,[1] A. Choudhury,[1] R. Hristu,[2] S. G. Stanciu,[2] and G. A. Stanciu[2]

[1]Nanoscience Laboratory, Department of Physics, Tezpur University, Assam 784 028, India
[2]Center for Microscopy-Microanalysis and Information Processing, University "Politehnica" of Bucharest, 060032 Bucharest, Romania

DOI: 10.1109/JPHOT.2010.2093513

Manuscript received September 28, 2010; revised November 9, 2010; accepted November 9, 2010. Date of publication November 18, 2010; date of current version December 7, 2010. This work was supported by the Department of Science and Technology (DST), Government of India, under Project SR/S5/NM33/2005 and the Ministry of Education and Research, Government of Romania, sanctioned by the project INT/ROMANIA/R-05/07 under the Indo-Romania joint program of cooperation. Corresponding author: D. Mohanta (e-mail: best@tezu.ernet.in).

Abstract: The fabrication and nonlinear optical imaging of ~5-nm-sized lead sulfide (PbS) nanoscale particles prepared in a water-soluble polymer matrix is reported. The two photon excitation fluorescence (TPEF) studies (using Ti:Sapphire laser, $\lambda_{ex} \sim 706$ nm, $P = 400$ mW, pulse ~80 fs) clearly show the foremost band-edge and asymmetric trap-related emissions. The chain-like organization of PbS nanoparticles was evident from the electron microscopy studies, and the impression from a cluster of nanopatterns was observable through laser scanning confocal microscopy. We have observed adequate correspondence between the TPEF spectra-based nonlinear optical images and spots corresponding to PbS nanoparticle assemblies. In addition, the PbS nanoparticles that are capable of producing strong second harmonic signals were efficiently imaged along the forward direction of the nonlinear microscopy. Investigation of two photon absorption processes along with the second-harmonic-generated imaging indicates the possibility of using the nanoscale particles in single molecule fluorescence spectroscopy, biomolecular labeling, and/or imaging applications.

Index Terms: Nanoparticles, luminescence, second harmonic generation (SHG), two photon excitation fluorescence (TPEF).

1. Introduction

In recent years, there has been a great deal of research interest in nanoscale narrow band gap semiconductors owing to the scope of tunable emission over a wide electromagnetic spectrum and the possibility of coupling with wide bandgap systems. Lead sulfide (PbS) is a narrow bandgap ($E_g \sim 0.41$ eV at 298 K) semiconductor system with comparable electron and hole effective masses ($m_e = 0.22\ m_0$; $m_h = 0.29\ m_0$), with m_0 being the rest mass of the free electron. As a semiconductor, its attraction lies in its large excitonic Bohr radius ($a_B \sim 18$ nm), as compared with other binary compounds [1]. Since the energy gap increases with decreasing crystallite size, nanoscale PbS could provide maximum tunable energy gap (nearly 10-fold value), compared with its bulk counterpart [2]. Further, PbS displays a broad emission response near the telecommunication wavelength ($\sim$1.56 μm). This emission response endows it with immense technological importance for application in fiber optic communication devices [3]. It has been predicted that the PbS nanoparticles

can be employed in the fabrication of infrared (IR) sensors and detectors [4]. PbS quantum dot doped glasses could also be used as saturable absorbers for solid state lasers [5]. Schmitt-Rink *et al.* have argued that the resonant nonlinear optical properties would be strongest for the nanocrystals of size (R) smaller than the bulk Bohr excitonic radius [6]. As PbS nanoparticles in the strong quantum confinement limit can be suitably fabricated with advanced synthesis protocols, it is better opted for various studies in the said regime. Nanoscale materials, in the strong confinement regime, could display resonantly enhanced optical nonlinearities and, thus, can become potential candidates for fast optical switching and information processing [7]. In order to use such quantum confined solids for lasing, frequency modulation, and bioimaging purposes, it is extremely important to explore upconversion of light, harmonic generation, and saturation absorption characteristics [8]. A pump laser can induce transient asymmetry in a molecular system that is capable of producing second-order nonlinear optical phenomena like second harmonic generation (SHG) [9], [10]. In a nanoscale PbS system, the noncentrosymmetry can be induced momentarily, leading to the excitation of dipoles that would oscillate in a way to give rise to SHG. The relaxation to the ground state from the excited states can be accompanied by the radiation of photons with frequency doubled. As far as nonlinear optical studies are concerned, earlier researchers have used either *z*-scan method [11] or four wave mixing technique [12] to determine nonlinear refractive index (consequently, nonlinear susceptibility) and in order to assess the figure of merit of the nonlinear device. Conversely, much attention has not been given to imaging fluorescent nanoparticles by direct excitation or via two photon excitation processes. Traditional fluorophors, e.g., organic dyes and fluorescent proteins, are limited by their narrow absorption range and broad emission spectra along with weak photostability. Observation of fluorescence from single PbS quantum dots using confocal microscopy [13] and water-soluble PbS quantum dots for *in vivo* biological imaging [14] that absorb and emit in the near-IR regime have been reported. Here, we discuss two photon absorption events and corresponding nonlinear optical imaging of surface passivated PbS nanocrystals using confocal laser scanning spectroscopy with Ti:Sapphire as the excitation source. A correlation of excited nanoparticles and spots depicting particle assemblies has also been highlighted.

2. Experimental Details: Materials and Methods

Over the years, glass [15], zeolite [16], and polymers [17] have been used by different workers to protect nanoparticles from agglomeration. Polymers are generally used as stabilizers, which controls the growth of nanoparticles inside the matrix. Acetonitrile is an organic solvent having a lone pair of electrons which forms a dative bond to the lead ions at the nanoparticle surface [18]. The effect of the bond strength to the nanoparticle surface can be ascertained by comparing the properties of the sulfur and nitrogen-bonded samples. Here, first, 5% polyvinyl alcohol (PVA) solution was prepared in the dark, and then, 0.1 M $PbCl_2$ solution was added to it with a matrix-to-aq. $PbCl_2$ volume ratio of 2 : 1, followed by vigorous stirring ($\sim$200 rpm) for 2 h. Then, drop wise injection of Na_2S in acidic medium was allowed until the precursor turned faint brown. During the reaction, GR-grade Acetonitrile was added to the above solution simultaneously. In this way, the PbS nanocrystals were encapsulated in a water-soluble dielectric media (PVA), while effective surface passivation was achieved by treatment with acetonitrile. The particle size and morphology are revealed from transmission electron microscopy (TEM), whereas nonlinear optical studies were carried out by laser scanning confocal microscopy.

Confocal microscopes allow only the signals from the focal plane for imaging and rejects all signals coming from planes beyond the focal plane, and thus, in-focus detail can be efficiently imaged through optical sectioning of planes [19]. A scheme of laser scanning configuration is shown in Fig. 1. For imaging based on two photon excitation fluorescence (TPEF) and SHG, we have used a confocal spectral laser scanning microscope (Model: Leica TCS SP) of power 400 mW. The objective has a magnification of 10$\times$ with 0.37 NA. We have used the IR port on the microscope for images corresponding to multiphoton excitation. The excitation source was a 80 fs pulsed, 80 MHz, Tsunami Ti:Sapphire laser, tunable in the range 700–850 nm but stabilized at $\sim$706 nm for the purpose of our experiment. For the multiphoton excited fluorescence, we collected

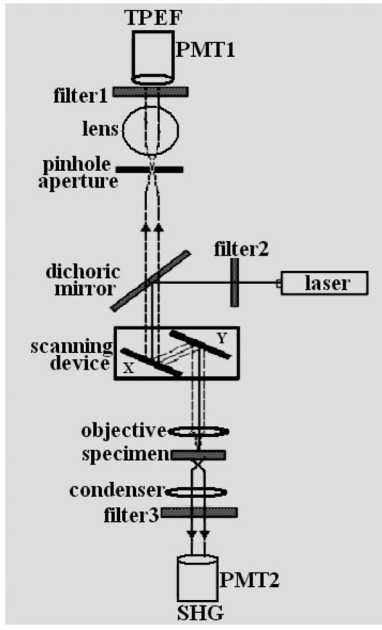

Fig. 1. Scheme of laser confocal microscope used for TPEF and SHG experiments.

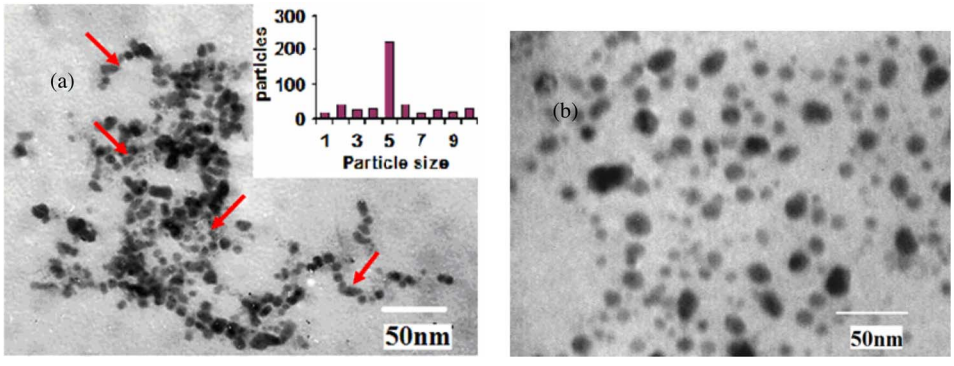

Fig. 2. TEM image of PbS nanoparticles dispersed in the polymer host (a) with and (b) without acetonitrile treatment. For case (a), the figure inset shows typical nanoparticle size distribution.

the optimum signal in the epi-direction (the backscattered signal) by appropriate pinhole adjustment. In SHG microscopy, the signal was collected in the forward direction i.e., along the direction of the incident beam (see Fig. 1).

While using the spectral confocal scanning microscope, the detector was first set for detecting at one wavelength, and then, the microscope was allowed to scan over a complete image frame of an optical section fixed at a particular depth to image the sample's fluorescence for the corresponding wavelength. Subsequently, the next fluorescence images from the same image-frame were detected by setting the detector to detect at consecutive wavelengths separated by a difference of 4 nm. Although the microscope had the provision for scanning image frames at different regions of the same optical section or another optical section at different depths of the sample, the images described in this work were taken at the same region for one particular optical section.

3. Results and Discussion

The transmission electron micrograph of synthesized PbS nanoparticles is shown in Fig. 2. It depicts the formation of quasi-spherical nanoparticles, a narrow size distribution with an average

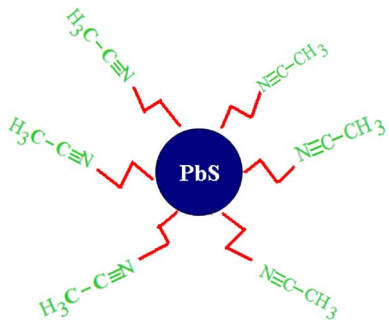

Fig. 3. Schematic of acetonitrile treated PbS nanoparticle.

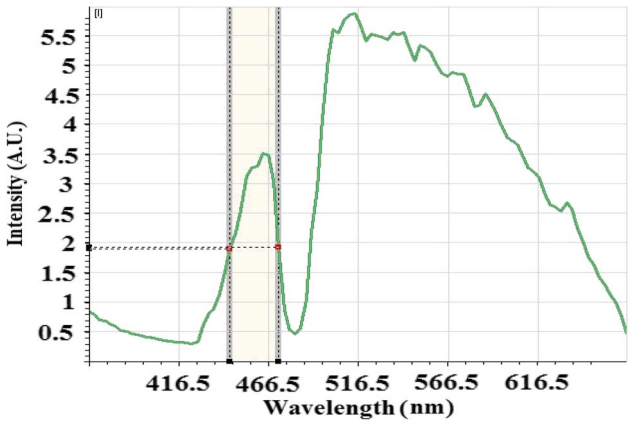

Fig. 4. Experimental TPEF spectra of surface passivated PbS nanoparticles.

nanoparticle size of ~5 nm and size dispersion of $4.3 \times 10^{11}/\text{cm}^2$. The particles are found to be unclustered and are in isolation from each other. The faint dark impressions are believed to be the image contrast of the nanoparticles lying on the underneath planes. Occasional instances of chain-like arrangements have also been noticed and are shown by arrow marks. Formation of such organized arrays is assigned to the interparticle interaction, owing to the unequal charge distribution, resulting in a strong dipole–dipole interaction for particles of varied sizes [20]. In addition, acetonitrile could have been strongly adsorbed on to the nanoparticle surface through its lone pair electron on the nitrogen, which has resulted in dominant surface passivation compared with dissolution [21]. Note that, in case of nanoparticle synthesis without acetonitrile treatment, we have not observed chain-like patterns [see Fig. 2(b)]. Earlier, it was known that acetonitrile is a polar, water soluble, and weakly reactive compound which is extensively employed as a displaceable ligand [22]. The nanoparticle surface containing dangling or unsaturated bonds can be passivated efficiently in view of the presence of lone pair of electrons located at the N-site of the acetonitrile (see Fig. 3). PbS quantum dot pairing as a result of charge manifestation events has been reported by our group only recently [23].

It is known that the TPEF is associated with the simultaneous absorption of two photons of the same or different energy and corresponds to the emission of a photon of energy higher than that of the absorbed photons [24]. The illustration of TPEF spectra along with respective images are presented in Figs. 4–6. The use of a near-IR as excitation source ($\lambda \sim 706$ nm) would reduce the unwanted scattering effect, whereas an extremely short pulse (~80 fs) facilitates simultaneous absorption of near-IR photons. The high power and short pulses of the laser source enforce the PbS nanoparticles to capture several photons simultaneously. The TPEF spectrum shows two distinct emission features. The first one is sharp, relatively symmetric, and peaking at ~466 nm with a full-width at half-maximum

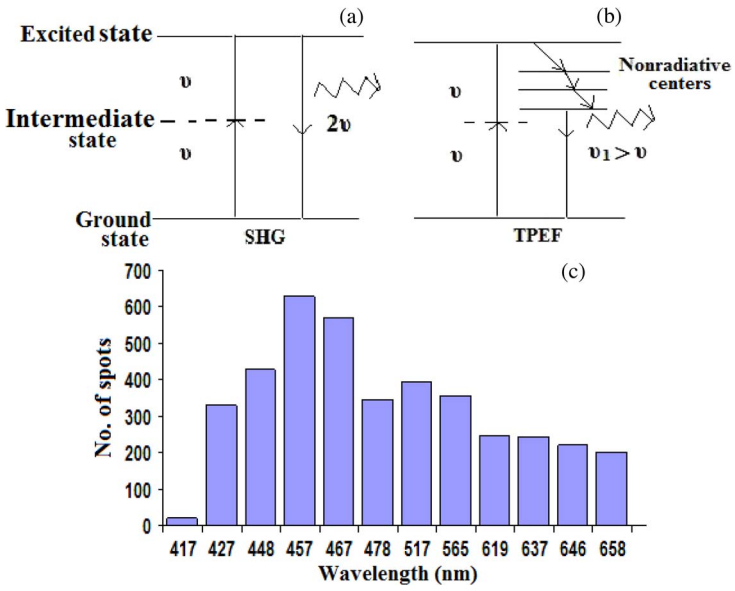

Fig. 5. Schematic of (a) SHG and (b) TPEF events and (c) TPEF emission with respect to the number of spots at different wavelengths.

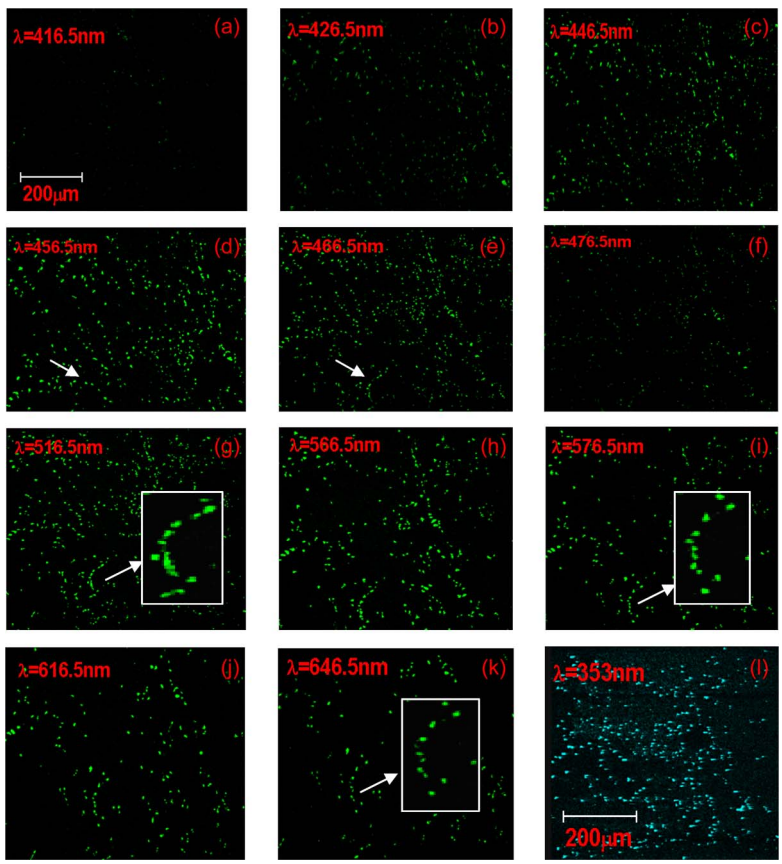

Fig. 6. (a)–(k). Fluorescence images of a specific region (1×1 mm^2) obtained as a result of TPEF process corresponding to different wavelengths. Fig. 6 (l) SHG image of the same region with signal collected in the forward direction. The figure insets in (g), (i), and (k) represent TPEF images from chain like assemblies of nanoparticles.

(FWHM) of ~0.408 eV and is ascribed to the band-edge emission [25]. In a typical fluorescence activation process, the band-edge emission peak corresponds to the highest energy [26]. The second band within 516.5–665.5 nm is a broad and asymmetric and represents defect-related emission. The surface traps on the nanoparticles would act as the nonradiative centers for subsequent retrapping and recombination emission. They supply some virtual intermediate (trap) states which could facilitate two photon emissions [27]. The asymmetry nature of the broadband could have arisen for one or more reasons, e.g., unequal energy spacing between subsequent surface traps within the forbidden energy gap [28], unequal probability of the radiative process via nonradiative pathways, and similar reasons based on size dependent effects.

The high resolution TPEF images are shown in Fig. 6, in which each of the images corresponded to the emission response of PbS nanoparticles, owing to the laser scanning area of 1×1 mm^2 at a designated wavelength. The first set of images [see Fig. 6(b)–(e)] are related to the near band-edge emission events. Referring to Fig. 4, the TPEF response is found to be weaker at the bottom and base parts [see Fig. 6(a), (b), and (f)] than the upper parts of the main peak [see Fig. 6(c), (d), and (e)]. Owing to the low scattering events of IR photons compared with the UV photons, use of IR photons is expected to provide high resolution imaging with adequate reproducibility, keeping the sample quality intact. In addition, they require higher damage threshold in a given focal volume of the specimen. In fact, the probability of fluorescence emission of inorganic fluorophor increases quadratically with the excitation intensity. With the average laser power of 400 mW and the beam diameter of ~1.2 μm, the incident power received at the sample was estimated to be ~0.0354 GW/cm^2. The laser wavelength was stabilized at 706 nm, and a pulse of duration $\Delta t \approx 80$ fs with a repetition rate of 80 MHz was used in the experiment, and therefore, every pulse was carrying as large as $\sim 1.15 \times 10^{14}$ photons altogether [29]. Such an intense beam would largely facilitate two photon absorption events. In a temporal overlap region of two pulses, the fluorescence will be much stronger over the FWHM range($\Delta z_{\mathrm{TPF-FWHM}}$) and $\Delta z = c\sqrt{2}\Delta t$, where c is the velocity of light [30]; in this case, Δz is found to be ~29.6 μm. Effectively, the probability of simultaneous photon absorption condition is adequately provided to each of the PbS nanoparticles.

Further, for nonlinear optical studies, we ensured that the experiment was performed in the safe-limit of the PbS system. The energy carried by each pulse ($\sim 3.2 \times 10^{-14}$ J) is relatively smaller than the critical value of the damage threshold energy ($E_{\mathrm{th}} = 353.9 \times 10^{-14}$ J) for the PbS system, as calculated using following equation [31]:

$$E_{\mathrm{th}} = \frac{I_{\mathrm{th}} \tau \lambda^2}{(NA)^2 + I_{\mathrm{th}} \frac{\lambda^2}{P_{cr}}} \tag{1}$$

with critical power given by

$$P_{cr} = \frac{3.77\lambda^2}{8\pi\, n_0 n_2'}. \tag{2}$$

Here, τ is the pulse duration, NA is the numerical aperture, λ is the laser wavelength, n_0 is the linear, and n_2' is the nonlinear refractive indices for PbS [32], [33]. In order to validate TPEF response of individual or cluster of particles, we calculated the number of isolated spots present in individual images Fig. 6(a)–(k). The wavelength versus number of distinct spots is shown in Fig. 5(c). With a nanoparticle size dispersion $\sim 4.3 \times 10^{11}/\mathrm{cm}^2$, and knowing the beam diameter ~1.2 μm, we predict that each of the pulse would enforce about 4860 particles to participate in the multiphoton absorption process. Since the TPEF signals were obtained by scanning over the sample of area 1×1 mm^2 and because of the fact that closely situated particles correspond to the interfering fluorescence, a maximum number of 630 impressive spots, corresponding to $\lambda_{\mathrm{em}} = 456.5$ nm, was observed [see Fig. 6(d)]. We argue here that each bright spot could be as a result of collective TPEF signals generated from many closely spaced independent PbS nanoparticles existing in assemblies. Depending on the arrangement and geometry of a particular assembly, we notice spots of varying

shape. The shape-asymmetry varies from oblate to triangular and rectangular to spheroidal, depending on the distribution of the constituent PbS nanoparticles in a given organization. Note the nonoverlapping chain-like distribution of spots and definite chain-like particle organization, as is evident in TEM studies. It is, therefore, ascertained that each of the isolated PbS nanoparticles within an organization is capable of fluorescing independently. The faint spots can be ascribed to the nanoparticle emission response in underneath planes. The two photon emission response, corresponding to $\lambda = 456.5$ nm, is characterized by the maximum number of spots which gradually decreases with increase in wavelength. Referring to the second band of the TPEF [see Figs. 4 and 5(c)], the number of spots observed has decreased from nearly 315 to 200 within an emission wavelength range 516.5–666.5 nm. It is possible that the closely spaced PbS nanoparticles within an organization (with spacing close to the lattice parameter) are losing energy initially through the nonradiative pathways and, finally, by abrupt emission of photons [see Fig. 6(g)–(k)] [34]. Owing to the large surface-to-volume ratio of the ultra small PbS nanoparticles ($\sim$5 nm), within organizations, there is a significantly higher probability of trap-related emissions compared with the band-edge emission, which is why we notice prominent TPEF signals in the former case.

Further along the forward direction, the encapsulated PbS nanoparticles are capable of producing significant second harmonic signals $(\lambda = 352$ nm$)$. We know that the efficiency of SHG depends on the phase matching condition ($\Delta \boldsymbol{k} = 0$, $\boldsymbol{k}$ being the propagation vector) [35], which is related to the phase coherence length L_c given by

$$L_c = \frac{\pi c}{2\omega(n_2 - n_1)} = \frac{\lambda}{4(n_2 - n_1)}. \tag{3}$$

In our experiment, taking $n_1 = 2.78$ and $n_2 = 4.56$ [36] as the refractive indices at the respective wavelengths of 352 nm and 706 nm, we have estimated L_c to be $\sim 10^{-7}$ m. Here, ω is the frequency analog of incident $\lambda = 706$ nm. Since the second harmonic power increases almost quadratically with particle dimension (d) smaller than the coherence length (L_c) [37], one could observe adequate SHG signals in the present case (with $d \sim 5$ nm and $L_c \sim 100$ nm).

The last image of Fig. 6 [labeled as (l)] represents SHG image obtained from the same PbS specimen. It depicts distribution of intense spots corresponding to the light emission feature of the isolated PbS nanoparticles, at half-wavelength (i.e., 353 nm) of the pump beam, and obtained along the forward direction. In addition, the TPEF is an incoherent process which can be observed in both the centrosymmetric and noncentrosymmetric systems and describes specific anisotropy, depending on the symmetric nature of the medium, whereas SHG is the signature of a crystalline noncentrosymmetric phase with a sensitivity down to several nanometer scale [38]. Due to incoherent radiation nature of TPEF process, we could obtain signals from the PbS nanoparticles over a large spectral range up to 670 nm with relevant imaging in the symmetric band-edge regime. The trap-related emission is associated with the nonradiative centers with uneven energy spacing and, hence, is observed as a broad asymmetric emission in the larger wavelength regime.

In case of SHG image, the number of spots (each corresponding to a nanoparticle assembly) is calculated to be 315, and the total number of nanoparticles is close to that were excited all at once by the ultra small laser pulse. A close look on the SHG image tells us that there is an impression of stretched bright spots that could be aroused due to temporal overlapping of single wavelength emission response from the adjacent nanoparticles. As the acetonitrile-treated $\sim$5 nm quasi-spherical particles can undergo surface charge oscillation under the influence of an intense em-field, there could be appreciable displacement of atoms that constitute a molecular solid. A slightest departure from the rock-salt symmetry allows the system to behave as noncentrosymmetric one. In other words, ultra small size, departure from the perfect spherical shape, and the use of an intense em-field along with surface treatments play major roles in inducing noncentrosymmetricity. As a result, isolated nanoparticles could display substantial SHG signals. Furthermore, PbS has a relatively higher refractive index value $(n_{\mathrm{PbS}} = 4.5)$ compared with the host polymer matrix

($n_{PVA} = 1.3$). Therefore, the materials will respond differently to the incident light, as per the equation $I = P/A = (n_0/2\mu_0 c)\ E^2$ with symbols have their usual meanings [39]. The situation can be equivalent to the case of presence of a dielectric sphere in a uniform electric field. Under the influence of a transient em-field, the interface separating the two media has a large field gradient ($\sim 9.3 \times 10^6$ V/cm), leading to the formation of dipoles on the surfaces of the PbS particles [40]. These dipoles would oscillate in such a way that the polarization so induced can vary with the applied field in a nonlinear way. Recently, strong Kerr signals as a result of transient anisotropy in a dispersed nanoparticle system have been reported by our group [41]. It was suggested that the even the low-power lasers could result in induced polarization that can lead to a transient anisotropy in the individual nanoparticles. In contrast, high power pulsed lasers are more promising for generating and detecting second harmonic signals when ideal conditions are met. Quantum dots were introduced to cell biology as alternative fluorescent probes in recent years. Earlier, PbS nanocrystals entrapped in the hollow core of apoferritin protein cages ensured the development of near-IR fluorescent composites [42]. Similarly, the use of PbS quantum dots as bioconjugates for near-IR contrast agents for targeted molecular imaging with expanded emission wavelengths beyond 1 μm has also been reported [43]. In this context, our TPEF and SHG results on PbS nanoparticles can be promising for imaging tissues, infected cells, and other such biological specimens.

4. Conclusion

We have shown that the acetonitrile-treated PbS nanoparticles could lead to chain-like ordering. The photoluminescence study through simultaneous photon absorption events reveals intense emission at $\sim$466 nm, depicting band-edge emission. Further, detectable TPEF and SHG signatures were witnessed for the synthesized nanoparticles. Each of the asymmetric spots obtained in the nonlinear optical imaging could have been aroused due to the interfering emission response of the closely spaced particles that exist in a given geometry. The TPEF spectra observed by us at room temperature open up the possibility of imaging and sensing nonfluorescent biomolecules that could make effective binding with such nanoparticles. Imaging by nonlinear spectroscopy can help in understanding the structure, organization, and conformational dynamics of the bioconjugates with high specificity. Consequently, more experiments on selective nanobioconjugate systems are necessary to substantiate two photon and multiphoton absorption events, with due emphasis on nanoparticle size-dependent processes.

References

[1] N. de la Rosa-Fox, R. Erce-Montilla, M. Pinero, and L. Esquivias, "Controlled size of PbS nanocrystals doped ORMOSIL," *Opt. Mater.*, vol. 22, no. 1, pp. 1–6, Mar. 2003.
[2] N. Belman, A. Berman, V. Ezersky, Y. Lifshitz, and Y. Golan, "Polarized photoluminescence from surface-passivated lead sulfide nanocrystals," *Nanotechnol.*, vol. 15, no. 1, pp. 16–22, Jan. 2004.
[3] K. K. Nanda, F. E. Kruis, H. Fissan, and M. Acet, "Band gap-tuning of PbS nanoparticles by in-flight sintering of size classified aerosols," *J. Appl. Phys.*, vol. 91, no. 4, pp. 2315–2321, Feb. 2002.
[4] A. A. Patel, F. Wu, J. Z. Zhang, C. L. Torres-Martinez, R. K. Mehra, Y. Yang, and S. H. Risbud, "Synthesis, optical spectroscopy and ultra fast electron dynamics of PbS nanoparticles with different surface capping," *J. Phys. Chem. B*, vol. 104, no. 49, pp. 11598–11605, Dec. 2000.
[5] B. Yu, G. Yin, C. Zhu, and F. Gan, "Optical nonlinear properties of PbS nanoparticles studied by Z scan method," *Opt. Mater.*, vol. 11, no. 1, pp. 17–25, Nov. 1998.
[6] S. Schmitt-Rink, D. A. B. Miller, and D. S. Chemla, "Theory of the linear and nonlinear optical properties of semiconductor micro crystallites," *Phys. Rev. B, Condens. Matter*, vol. 35, no. 10, pp. 8113–8125, May 1987.
[7] F. W. Wise, "Lead salt quantum dots: The limit of strong quantum confinement," *Acc. Chem. Res.*, vol. 33, no. 11, pp. 773–780, Aug. 2000.
[8] A. P. Alivisatos, "Perspectives on the physical chemistry of semiconductor nanocrystals," *J. Phys. Chem.*, vol. 100, no. 31, pp. 13226–13239, Aug. 1996.
[9] J.-M. Nunzi, F. Charra, C. Fiorini, and J. Zyss, "Transient optically induced non-centrosymmetry in a solution of octupolar molecules," *Chem. Phys. Lett.*, vol. 219, no. 5/6, pp. 349–354, Mar. 1994.
[10] B. Sahraoui and I. V. Kityk, "Mid-infrared light-induced second-harmonic generation in specific glasses," *J. Opt. A: Pure Appl. Opt.*, vol. 5, no. 3, pp. 174–179, May 2003.
[11] A. I. Ryasnyansky and B. Palpant, "Theoretical investigation of the off-axis z-scan technique for nonlinear optical refraction measurement," *Appl. Opt.*, vol. 45, no. 12, pp. 2773–2776, Apr. 2006.

[12] G. Fu, T. Yoda, K. Kasatani, H. Okamoto, and S. Takenaka, "Third-order optical nonlinearities of naphthalocyanine derivatives measured by resonant femtosecond degenerate four-wave mixing technique," *Synthetic Metals*, vol. 155, no. 1, pp. 68–72, Oct. 2005.
[13] J. J. Peterson and T. D. Krauss, "Fluorescence spectroscopy of single lead sulfide quantum dots," *Nano Lett.*, vol. 6, no. 3, pp. 510–514, Mar. 2006.
[14] L. Bakueva, I. Gorelikov, S. Musikhin, X. S. Zhao, E. H. Sargent, and E. Kumacheva, "PbS quantum dots with stable efficient luminescence in the near-IR spectral range," *Adv. Mater.*, vol. 16, no. 11, pp. 926–929, Jun. 2004.
[15] T. Okuno, A. A. Lipovskit, T. Ogawa, I. Amagai, and Y. Masumoto, "Strong confinement of PbSe and PbS quantum dots," *J. Lumin.*, vol. 87–89, no. 1/2, pp. 491–493, May 2000.
[16] K. Moller, T. Bein, N. Herron, W. Mahler, and Y. Wang, "Encapsulation of lead sulfide molecular clusters into solid matrixes," *Inorg. Chem.*, vol. 28, no. 15, pp. 2914–2919, Jul. 1989.
[17] Z. Qiao, Y. Xie, M. Chen, Y. Xu, Y. Zhu, and Y. Qian, "Synthesis of lead sulfide/(polyvinyl acetate) nanocomposites with controllable morphology," *Chem. Phys. Lett.*, vol. 321, no. 5/6, pp. 504–507, May 2000.
[18] S. A. Majetich and A. C. Carter, "Surface effects on the optical properties of cadmium selenide quantum dots," *J. Phys. Chem.*, vol. 97, no. 34, pp. 8727–8731, Aug. 1993.
[19] S. J. Hewlett and T. Wilson, "Resolution enhancement in three dimensional confocal microscopy," *Mach. Vis. Appl.—Special Issue: Three-Dimensional Microscopy*, vol. 4, no. 4, pp. 233–242, Sep. 1991.
[20] Z. Tang, A. N. Kotov, and M. Giersig, "Spontaneous organization of single CdTe nanoparticles into luminescent nanowires," *Science*, vol. 297, no. 5579, pp. 237–240, Jul. 2002.
[21] F. B. Li, H. Bremner, and A. E. Burgess, "Dissolution and passivation of iron in acetonitrile and acetonitrile–water mixtures," *Corros. Sci.*, vol. 41, no. 12, pp. 2317–2335, Dec. 1999.
[22] S. Kelvin and Z. Y. Leung, "Synthesis, structural characterisation and electrochemistry of a heptaosmium carbonyl cluster bearing a dppf moiety: Crystal and molecular structure of $[Os_7(CO)_{17}(\mu_4 - \eta^2 - CO)(MeCN)(\mu - dppf)]$," *Inorg. Chem. Commun.*, vol. 2, no. 10, pp. 498–502, Oct. 1999.
[23] D. Mohanta, H. Bora, N. Dutta, and A. Choudhury, "Development principles and production of paired PbS quantum dots," *Eur. Phys. J. Appl. Phys.*, vol. 41, no. 2, pp. 129–132, Feb. 2008.
[24] L. Pålsson, R. Pal, B. S. Murray, D. Parker, and A. Beeby, "Two-photon absorption and photoluminescence of europium based emissive probes for bioactive systems," *Dalton Trans.*, vol. 48, pp. 5726–5734, 2007.
[25] H. Cao, G. Wang, S. Zhang, and X. Zhang, "Growth and photoluminescence properties of PbS nanocubes," *Nanotechnol.*, vol. 17, no. 13, pp. 3280–3287, Jul. 2006.
[26] J. Hu, L.-S. Li, W. Yang, L. Manna, L.-W. Wang, and A. P. Alivisatos, "Linearly polarized emission from colloidal semiconductor quantum rods," *Science*, vol. 292, no. 5524, pp. 2060–2063, Jun. 2001.
[27] S. M. Zhuo, J. X. Chen, T. S. Luo, H. L. Chen, and J. J. Zhao, "High-contrast multimodel nonlinear optical imaging of collagen and elastin," *J. Phys.: Conf. Ser.*, vol. 48, pp. 1476–1481, 2006.
[28] C. Katan, S. Tretiak, M. H. Werts, A. J. Bain, R. J. Marsh, N. Leonczek, N. Nicolaou, E. Badaeva, O. Mongin, and M. Blanchard-Desce, "Two-photon transitions in quadrupolar and branched chromophores: Experiment and theory," *J. Phys. Chem. B*, vol. 111, no. 32, pp. 9468–9483, Aug. 16, 2007.
[29] J. Wilson and J. Hawkes, *Optoelectronics: An Introduction*. Harlow, U.K.: Pearson, 1998, pp. 169–241.
[30] W. H. Glenn, "Theory of the two-photon absorption-fluorescence method of pulse measurement," *IEEE J. Quantum Electron.*, vol. QE-6, no. 8, pp. 510–515, Aug. 1970.
[31] C. B. Schaffer, A. Brodeur, and E. Mazur, "Laser-induced breakdown and damage in bulk transparent materials induced by tightly focused femtosecond laser pulses," *Meas. Sci. Technol.*, vol. 12, no. 11, pp. 1784–1794, Nov. 2001.
[32] R. Xie, D. Li, D. Yang, and M. Jiang, "Surface synthesis of PbS nanoparticles on silica spheres by a sonochemical approach," *J. Mater. Sci.*, vol. 42, no. 4, pp. 1376–1380, Feb. 2007.
[33] C. Li, G. Shi, H. Xu, S. Guang, R. Yin, and Y. Song, "Nonlinear optical properties of the PbS nanorods synthesized via surfactant-assisted hydrolysis," *Mater. Lett.*, vol. 61, no. 8/9, pp. 1809–1811, Apr. 2007.
[34] A. M. Agal'tsov, V. S. Gorelik, and I. A. Rakhmatullaev, "Spectral, energy, and temporal characteristics of two-photon-excited fluorescence of ZnSe single crystal in the blue region of the spectrum," *Semiconductors*, vol. 31, no. 12, pp. 1228–1230, Dec. 1997.
[35] R. Menzel, *Photonics*. New Delhi, India: Springer-Verlag, 2004, p. 161.
[36] [Online]. Available: http://www.filmetrics.com/refractive-index-database/PbS/Lead-Sulfide
[37] A. Ghatak and K. Thyagarajan, *Optical Electronics*. New Delhi, India: Cambridge Univ. Press, 1996, p. 574.
[38] S. Brasselet, V. Le Floc'h, F. Treussart, J. F. Roch, and J. Zyss, "*In situ* diagnostics of the crystalline nature of single organic nanocrystals by nonlinear microscopy," *Phys. Rev. Lett.*, vol. 92, no. 20, pp. 207 401–207 404, May 2004.
[39] A. Ghatak and K. Thyagarajan, *Introduction to Fibre Optics*. New Delhi, India: Cambridge Univ. Press, 1999.
[40] D. J. Griffiths, *Introduction to Electrodynamics*. New Delhi, India: Prentice-Hall, 1999.
[41] D. Mohanta, S. Biswas, and A. Choudhury, "Strong Kerr-signals from optically isotropic ZnSe nanocrystals: A study using Mach–Zehnder principles," *Eur. Phys. J. D*, vol. 55, no. 3, pp. 679–683, Dec. 2009.
[42] J. Sun, M. Zhu, K. Fu, N. Lewinski, and R. A. Drezek, "Lead sulfide near-infrared quantum dot bioconjugates for targeted molecular imaging," *Int. J. Nanomed.*, vol. 2, no. 2, pp. 235–240, 2007.
[43] B. Hennequin, L. Turyanska, T. Ben, A. M. Beltran, S. I. Molina, M. Li, S. Mann, A. Patane, and N. R. Thomas, "Aqueous near-infrared fluorescent composites based on apoferritin-encapsulated PbS quantum dots," *Adv. Mater.*, vol. 20, no. 20, pp. 3592–3596, Oct. 2008.